Power System Technology **Volume 46 · Number 4 · 2022**
ISSN: 1000-3673

Detection and Analysis of Insulation Aging State of AC 500 kV XLPE Submarine Cable Based on High Voltage Frequency Dielectric Response

Hao J., Dai X., Gao Z., Jian Z., Zheng X., Peng W.
1. China National Gold Group Co., Ltd., Beijing 100083, China
2. School of Civil and Resource Engineering, University of Science and Technology Beijing, Beijing 100083, China

ABSTRACT
To explore the influences of microwave irradiation on the mechanical response mechanism of rock under different confining pressures, granite specimens were subjected to different microwave heating paths, then conventional triaxial compression experiments were conducted. The experimental results show that: 1) As microwave irradiation power and time increase, the density and P-wave velocity of the specimen show a downward trend and the higher the power, the faster the decline; 2) The sensitivity of specimen strength to confining pressure and microwave (power and time) is ranked thus (in descending order): confining pressure, microwave power, then irradiation time. Under a low confining pressure, the strength value of the specimen exhibits a decreased trend with the increase of irradiation time, but with the increase of confining pressure, the change of the strength of the specimen tended to be consistent; 3) The strain energy evolution of the specimen is similar, it is mainly manifested in energy accumulation before the peak, and energy dissipation and release thereafter. Under the influence of microwave radiation, the evolution of dissipation ratio shows a significant microwave effect, but the microwave effect becomes weaker with the increase of confining pressure. Therefore, when using microwave rock-breaking techniques, combined with necessary pressure-relief technique, microwave irradiation can produce the best rock-breaking effect.

1. INTRODUCTION

In the process of deep metal resource mining, mining engineers are generally faced with deep stratigraphic dense, hard, strongly wear-resistant, and difficult to drill rock media which restrict the efficiency of deep mining. Therefore, research into deep hard rock breaking methods is a key technology to be tackled urgently at present. At present, the common rock-breaking methods used in mining are drilling and blasting methods and mechanical rock breaking, which account for more than 90% of output [1]. The drilling and blasting methods use the huge energy released instantly by explosives to break the rock. The advantage is incomparable in large rock crushing projects, but the drilling and blasting methods cause severe disturbance to the original rock, especially in a deep, high-stress environment where they readily cause damage to the adjacent surrounding rock body, and there are disadvantages such as low construction accuracy and difficulties in support of openings.

The mechanical rock breaking method can avoid the disadvantages of drilling and blasting methods through cutting, punching, rolling, grinding, and other techniques [2], but faces same problems such as the need for expensive mechanical equipment and tools, severe tool loss (especially crushing rock with a compressive strength of above 200 MPa), large maintenance investment, and other issues [1].

The shortcomings of mechanical rock-breaking techniques have led domestic and foreign scholars to introduce some new rock-breaking techniques to assist rock-breaking in the past 40 years, such as thermal karst, laser rock breaking, plasma rock breaking, microwave rock breaking [3-6], particle impact rock breaking, etc. [7-8], among which microwave rock breaking techniques have great application prospects [9-10]. The essence of microwave rock-breaking is that a large number of randomly distributed dipole molecules are present inside the rock, and under the mutual coupling of microwave electromagnetic fields, these dipole molecules oscillate at a frequency of hundreds of millions of cycles per second. As the dipole molecules have to overcome intermolecular interference and generate intense friction, electrical energy is converted into dielectric heat energy [11-13]. However, there are differences in the coefficients of thermal expansion of minerals in the rock, which generates thermal stress in the mineral grain boundary or within each grain, and when stress reaches or exceeds the strength of the rock, it will induce intergranular fracture or transgranular fracture among the minerals, damaging the rock, thus reducing its strength and wear resistance [7].

Scholars have conducted many studies on the effects of microwave irradiation on the mechanical properties of rocks, mainly uniaxial compressive strength [14-18], tensile properties [19], point load strength [20], and Debang index [21-22]. Lu et al. [15-16] used microwave irradiation in experiments on basalt and found that the higher the microwave radiation power and the longer the irradiation time, the faster the P-wave velocity and uniaxial compressive strength will be reduced. Hassani et al. [19-20] placed norite, granite, and basalt in a multi-mode cavity for microwave treatment when wave irradiation power was 1.2, 3, and 5 kW and the irradiation time ranged between 0 and 120 s. The experimental results found that the tensile strength and compressive strength decreased with the increase in microwave input energy. The higher the input microwave energy, the greater the reduction in strength. Dai et al. [23] conducted different microwave heating treatments on granite, and through the Brazilian disc experiment found that, at the same irradiation time, the higher power applied, the greater the decrease in strength and the more severe the damage; under the same irradiation power, the strength decreased more slowly with prolonged irradiation time. In addition, many scholars have explored the principle of microwave rock breaking from the perspective of rock mineral species [24-25], particle size [26], and water saturation [27].

In summary, microwave irradiation time and irradiation power are important parameters that influence the mechanical properties of rocks, but scholars have mostly concentrated on the effect of microwave irradiation on the unidirectional stress state of rock. However, in the actual mining and excavation process, the rock mass evolves from the working face along the radial direction to greater depth: the stress state changes from uniaxial, through biaxial, to triaxial [28], and the mechanical response of the rock mass is closely related thereto. Therefore, the author conducted conventional triaxial compression experiments on granite samples irradiated by microwaves to explore the effect of microwave irradiation on the mechanical properties of the rock under a triaxial state of stress. Meanwhile, because the nature of deformation and damage in loaded rocks is the result of the combined action driven by energy dissipation and energy release [29], combining the thermodynamic perspective to study the effect of microwave irradiation on the changing pattern of rock mechanical properties is closer to the essence of the problem. It can enrich the understanding of the mechanical behavior of rocks by microwave irradiation.

2. TEST PROGRAMME

2.1. Equipment

An RWLM6 microwave muffle furnace was used to process granite specimens under different irradiation powers for different times. The system uses a special industrial-grade microwave source, which can realize continuous and stable heating; the microwave output power is 6.5 kW, and the power is continuously adjustable from 0.1 to 6.49 kW, and the microwave frequency is 2.45 GHz ± 25 MHz: the experimental device is illustrated in Fig. 1.

Fig. 1 RWLM6 microwave high-temperature heating furnace

The experimental axial loading system uses Changchun Rising Sun TAW-2000 microcomputer electro-hydraulic servo-motor controlled triaxial experimental machine, the maximum axial load is 2000 kN, and the effective measurement range is 2% to 100% of the maximum axial pressure. The experimental radial loading device is a portable self-sealing rock triaxial experimental high-pressure chamber. It was developed and designed by the Key Laboratory of Ministry of Education for Efficient Mining and Safety of Metal Mines, University of Science and Technology Beijing. The device mainly consists of four subsystems: a high-pressure chamber, high-precision oil pressure control system, three-way valve, and ultra-high pressure hand pump. The loading equipment used in the experiment is shown in Fig. 2.

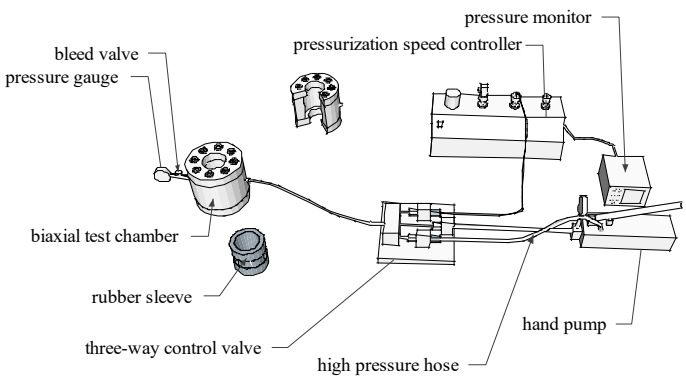

(a) Portable self-sealing rock triaxial experimental high-pressure chamber

(b) TAW-2000 electro-hydraulic triaxial testing machine

Fig. 2 TAW-2000 electro-hydraulic triaxial testing machine and triaxial high pressure chamber

2.2. Specimen preparation

The experimental specimens were formed from a piece of granite with uniform texture and no fractures, and the specimens measured Φ 30 mm × 60 mm (60 specimens were made). After measurement, the average density of the specimens was found to have been 2.68 g/cm3 at room temperature, and the P-wave velocity was 6.326 km/s. The flatness of the end face of the prepared sample was controlled to within ± 0.05 mm, and the perpendicularity of the end face to the axis did not exceed 0.25°. A photograph of a specimen after processing is shown in Fig. 3.

Fig. 3 A specimen after processing

2.3. Heating paths and loading paths

In the experiment, two heating paths were designed for microwave heating (Table 1).

Table 1 Microwave heating path

Heating path	Irradiation power(kW)	Irradiation time (min)	Experiment number
I	1	1	A
		3	B
		5	C
II	5	1	D
		3	E
		5	F

After the sample was processed according to the designed heating path, it was removed after standing for five minutes in the microwave heating furnace; it was allowed to cool to normal temperature in the laboratory. The quality, diameter, height, P-wave velocity, and conventional triaxial compression strength of the sample after microwave heating were measured. To avoid discreteness affecting the measured results, the mean average value was taken after each test had been repeated three times.

Three of confining pressures (0 MPa, 10 MPa, and 20 MPa) were used: loading was applied in a radial and axial alternate loading mode. That is, the confining pressure was increased to 5 MPa, and then the axial pressure was increased to the hydrostatic pressure (the confining pressure increment was 5 MPa each time), until the confining pressure reached to the design pressure, the axial load was applied at a cross-head displacement rate of 0.02 mm/min until the sample was destroyed.

3. ANALYSIS OF EXPERIMENTAL RESULTS AFTER MICROWAVE IRRADIATION

3.1. Density change

Fig. 4 shows the density change of each specimen group before and after microwave irradiation.

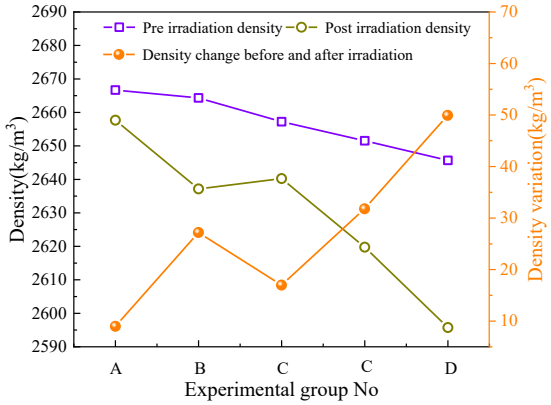

Fig. 4 Change of sample density before and after microwave irradiation

It can be seen from the figure that with the increase of irradiation power, the rate of change of specimen density is initially slow, then increased rapidly. At low power, the density decreases slightly over time at a given applied power: the density changes by 8.99 kg/m3 and 16.99 kg/m3 at 1 kW for 1 min and 1 kW for 5 min, respectively. At high power, the irradiation time has a significant effect on the density of granite: the density changes by 31.80 kg/m3 and 49.93 kg/m3 at 5 kW for 1 min and 5 kW for 3 min, respectively. This shows that, when the irradiation power is low, the influence of the irradiation power on the density of the granite is greater than the influence of the irradiation time, and the irradiation time exerts a greater effect on the granite as the power is increased. It is worth noting that the sample irradiated at 5kW for 5 min was molten by microwave irradiation, so no data were captured (Fig. 5).

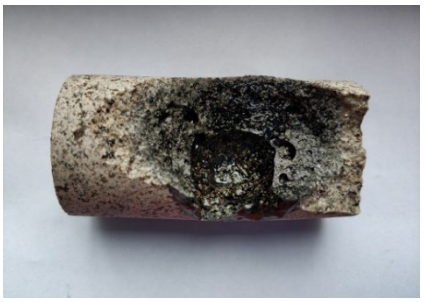

Fig. 5 Rock sample melting under microwave irradiation at 5 kW for 5 min

3.2. P-wave velocity

After the experimental specimens were irradiated by microwave, the relationship between P-wave velocity and microwave irradiation time and power was established (Fig. 6).

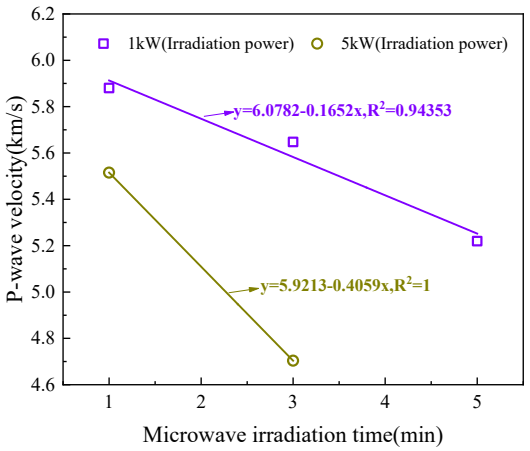

Fig. 6 Relationship between wave velocity and microwave irradiation time

As can be seen from Fig. 6, the wave velocity of the sample after microwave heating is less than the average value before heating, but there are significant differences in wave velocity under different heating regimes. Under the same microwave irradiation time, the higher the power, the more rapid the decline in P-wave velocity. For example, when the power is 1 kW

and 5kW, the absolute values of the slope are 0.1652 and 0.4059 respectively. This is because, at low power, the temperature of minerals in the sample rises slowly, allowing time for greater heat transfer and a smaller thermal stress difference.

4. ANALYSIS OF EXPERIMENTAL RESULTS AFTER MICROWAVE IRRADIATION

4.1. Stress-strain curves

The triaxial stress-strain curves of the granite specimens under different microwave irradiation paths are shown in Fig. 7: the triaxial compression stress-strain curves of the granite specimens after microwave heating evolve in a similar manner, all passing through an initial fracture compaction closure stage, linear elastic deformation, stable crack development, unstable crack development, and a post-peak stage.

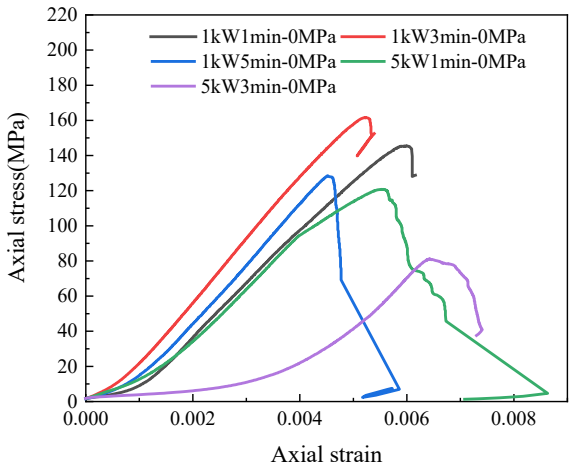

(a) σ2 = σ3 = 0 MPa

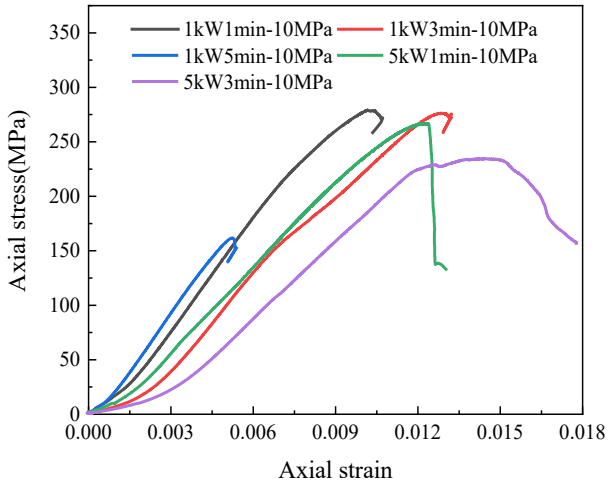

(b) σ2 = σ3 = 10 MPa

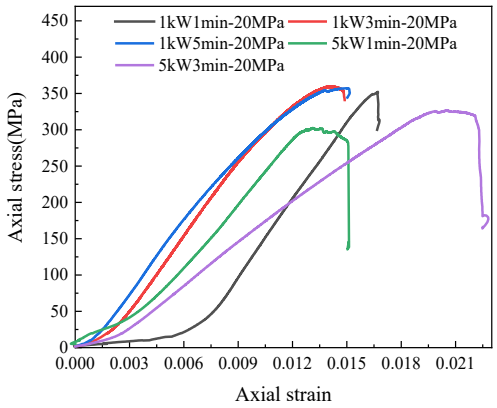

(c) σ2 = σ3 = 20 MPa

Fig. 7 Stress-strain curves of specimens under triaxial compression

Fig. 7 shows that the stress-strain curves of the specimens under different confining pressures exhibit the following variability: (1) at σ2 = σ3 = 0 MPa, influenced by the irradiation time and power, the 5 kW for 1 min specimen is similar to those in specimens irradiated at 1 kW, but the increasing trend of stress is significantly slower with the increase of strain before the peak; while the compaction stage of the 5kW for 3 min specimen is significantly longer than in other specimens, and the strength is significantly lower than under other heating paths, indicating that there is a critical value of microwave radiation damage to granite; (2) The stress-strain curves of the specimens are similar at σ2 = σ3 = 10 or 20 MPa. The cracks induced by the thermal stress reclose under the action of high confining pressure, and the original structural damage is effectively "repaired", which also reflects the fact that, as the confining pressure is increased, the critical value of microwave radiation on radiation-induced damage also increases.

4.2. Triaxial compressive strength

Under the action of different confining pressures, the strength changes in rock specimens under different microwave heating paths are shown in Fig. 8.

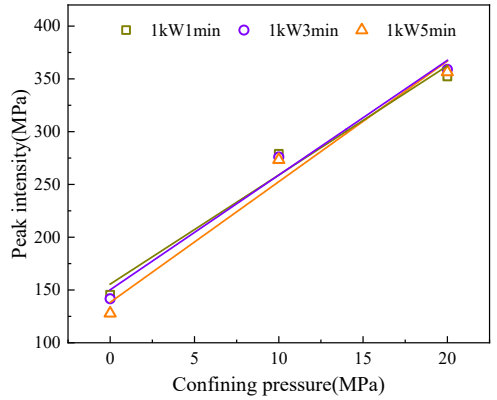

(a) Microwave heating path 1

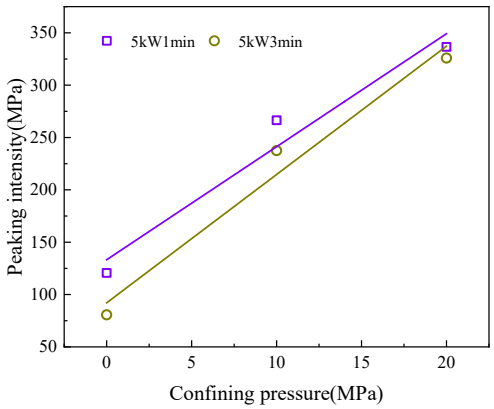

(b) Microwave heating path 2

Fig. 8 Triaxial compressive strengths of granite samples under different microwave heating paths

4.3. Deformation characteristics

Under different confining pressures, the relationship between the axial strain at the peak strength of the specimen (denoted by ε_{tcs}) and the irradiation time is shown in Fig. 9. It can be seen from the figure that, under all tested confining pressure, the value of ε_{tcs} of specimens with irradiation power of 5 kW increases to different extents as the irradiation time is increased from 1 min to 3 min. For example, at confining pressures of 0, 10, and 20 MPa, the increase in the value of ε_{tcs} is 0.086%, 0.26%, 0.89%, that is, the larger the confining pressure the greater the increase in ε_{tcs}. The internal structural damage under 5 kW for 3 min reaches a certain critical value, so the expansion of old cracks and the initiation of new cracks are fully developed under the action of a high confining pressure and the longer the pre-peak compression and fracture expansion stage. The ε_{tcs} value of the specimens irradiated at 1 kW decreases linearly at a confining pressure of 0 MPa, while fluctuates differently at 10 MPa and 20 MPa, indicating that, under the action of a high confining pressure, the sensitivity of ε_{tcs} to the confining pressure is greater than the influence thereof at low power. It is noteworthy that the values of ε_{tcs} for 1 kW 5 min specimens and 5 kW 1 min specimens at all tested confining pressures are similar.

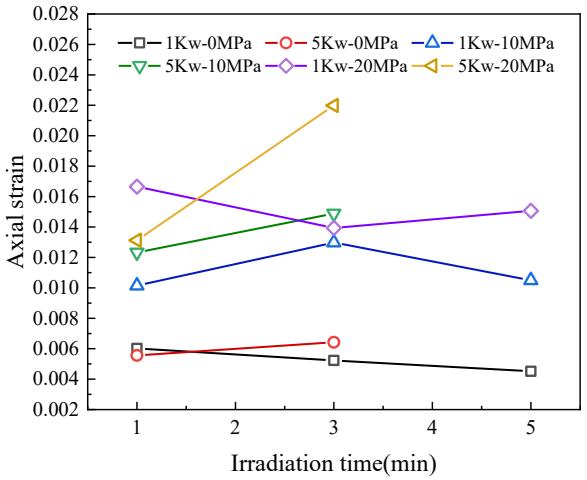

Fig. 9 Relationship between irradiation time and axial strain

5. CHARACTERISTICS OF ROCK ENERGY EVOLUTION UNDER TRIAXIAL COMPRESSION

5.1. Energy calculation method

Rock deformation and failure is the result of the combined effects of energy accumulation, dissipation, and release [30]. Assuming that the influence of heat generated by ambient temperature is not considered, when energy is input to the rock system from the outside, part of the energy is stored inside the rock as elastic deformation energy, and the rest is dissipated via plastic deformation, frictional heat, surface energy, etc. Taking into account the differences in the proportions of various measures of energy in the process of rock failure, we focus on analyzing the relationship between the total external input energy, elastic deformation energy, damage energy, and plastic properties (or dissipated energy), thereby revealing the influences of microwave irradiation and confining pressure on the energy evolution mechanism of granite.

The process of rock deformation to failure is assumed to be a closed system, and there is no heat exchange with the outside world. Then from the first law of thermodynamics, we obtain:

$$U^o = U^e + U^d \tag{1}$$

where, U^o is the work done by the experimental machine on the rock sample. Ue represents the elastic deformation energy accumulated in the rock sample. U^d denotes the dissipated energy, which mainly includes the damage energy of crack initiation and expansion and the plastic properties of mineral particles.

According to the two-way reversibility of the elastic deformation energy of the loaded rock mass, the one-way irreversibility of the dissipated energy, the characteristics of the rock stress-strain curve can be used to calculate the elastic energy and dissipated energy under any stress state on the curve, as shown in Fig. 10.

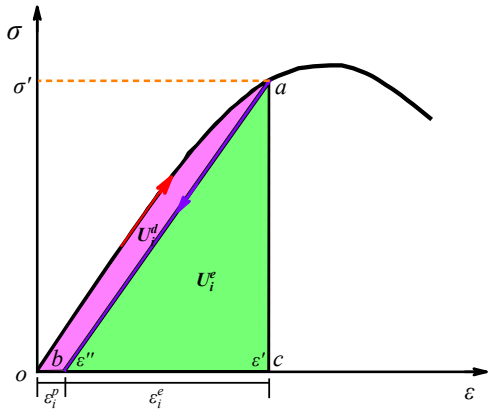

Fig. 10 Rock loading to σ′: energy calculation diagram

When the rock is loaded in the i-direction for time a, the total work done by the testing machine on the rock sample is the area oac; the elastic deformation energy represents the area of the region abc; dissipated energy is the area of the area oab, as shown in equation (2):

$$\begin{cases} U_i^o = \int_0^{\varepsilon'} \sigma_i d\varepsilon_i \\ U_i^e = \int_{\varepsilon''}^{\varepsilon'} \sigma_i d\varepsilon_i \\ U_i^d = \int_0^{\varepsilon'} \sigma_i d\varepsilon_i - \int_{\varepsilon''}^{\varepsilon'} \sigma_i d\varepsilon_i \end{cases} \tag{2}$$

In compression tests, the hoop deformation of the rock sample under the confining pressure is fixed, making the hoop energy much smaller than the change in axial energy. Therefore, the energy evolution in the ring direction is not considered when calculating the energy in the present work.

5.2. Analysis of energy conversion mechanism

According to the calculation method embodied by formula (2), the energy evolution curves of the granite specimen in the conventional triaxial compression process were obtained (Fig. 11): the energy evolution in the specimen can be roughly divided into two stages: pre-peak and post-peak. (1) Pre-peak stage: As the total external input energy continues to increase, elastic energy increases at a similar growth rate, and elastic energy accounts for more than 80% of the total. The other part of the energy that is mainly manifested as energy dissipation s used for initial crack closure during the compaction stage. It can be used for crack initiation, propagation, and plastic deformation of mineral particles during the transition from the stable to unstable crack-growth stage: the greater the confining pressure, the greater the energy consumption at that stage. (2) Post-peak stage: the growth rate of the total external energy input decreases, the elastic energy drops rapidly, and that dissipated increases rapidly. When unconfined, as the microwave irradiation damages the rock sample, the elastic energy drops more slowly after the peak. When the confining pressure is 10 MPa and 20 MPa, the rate of change (post-peak) after high-power irradiation becomes slower, and it changes positively with increasing confining pressure.

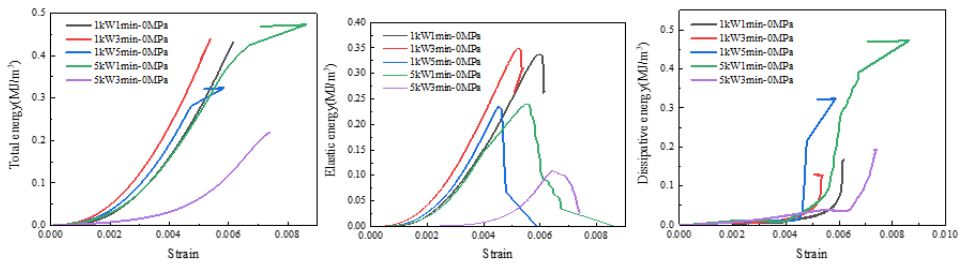

(a) σ2 = σ3 = 0 MPa

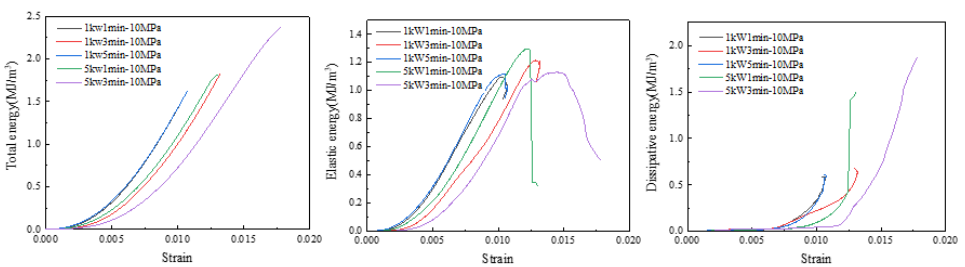

(b) σ2 = σ3 = 10 MPa

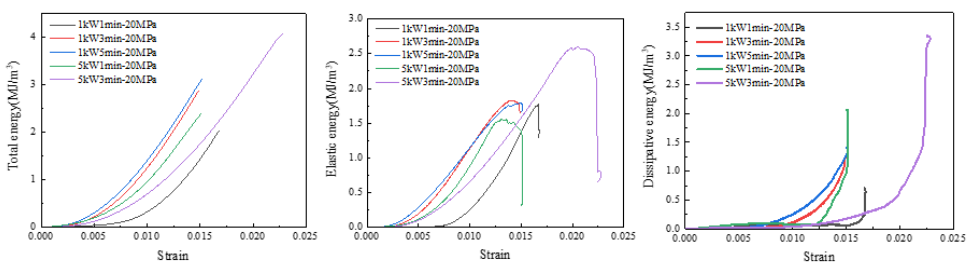

(c) σ2 = σ3 = 20 MPa

Fig. 11 The relationship between energy and strain under different confining pressures

5.3. Energy dissipation analysis

To reduce the influence of the discreteness of the specimens on the analysis results, the ratio of the dissipation energy of each specimen to the total input energy (i.e., the ratio is defined as the dissipation ratio) was used for analysis (Fig. 12).

It can be seen from the figure that, as the axial strain increases, the dissipation ratio generally shows a tendency to a “rapid increase-slow decrease-slow increase-rapid increase”. It is found by comparison that when the confining pressure is 0 MPa, the 5 kW 3 min specimens account for 86% of the entire deformation at failure during the “rapid rise-slow decline” stage. Under confining pressures of 10 MPa and 20 MPa, the evolution of the dissipation ratios of the specimens is highly similar, and the “rapid rise-slow fall” phases account for about 53% and 54% thereof. In the post-peak failure stage, the greater the damage, the slower the rise of the dissipation energy ratio, indicating that the energy release from the granite becomes slower after microwave irradiation, and the rock mass is weakened.

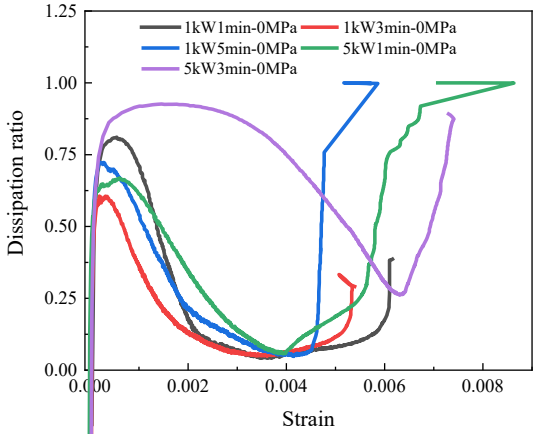

(a) σ2 = σ3 = 0 MPa

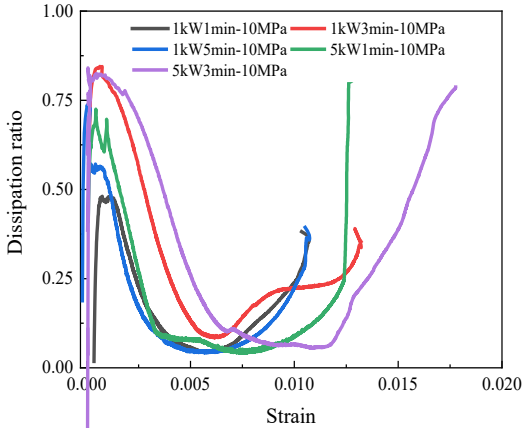

(b) σ2 = σ3 = 10 MPa

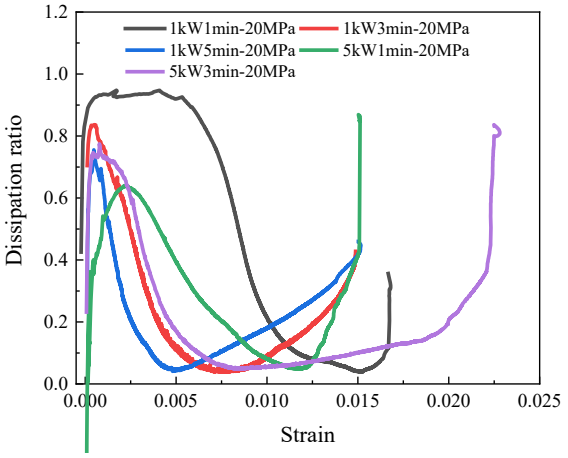

(c) σ2 = σ3 = 20 MPa

Fig. 12 Relationship between dissipation ratio and strain under different confining pressures

5.4. Characteristic energy analysis

To quantify the influences of the microwave heating path on the evolution of the strain energy of rock samples under different confining pressures, the energy storage limit (maximum elastic energy), residual elastic energy, and maximum dissipation energy were used for analysis (Fig. 13).

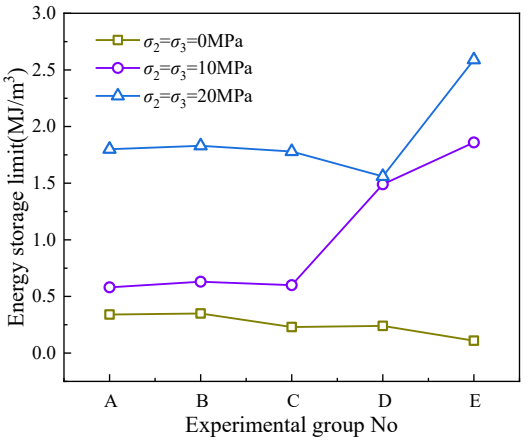

(a) Energy storage limit

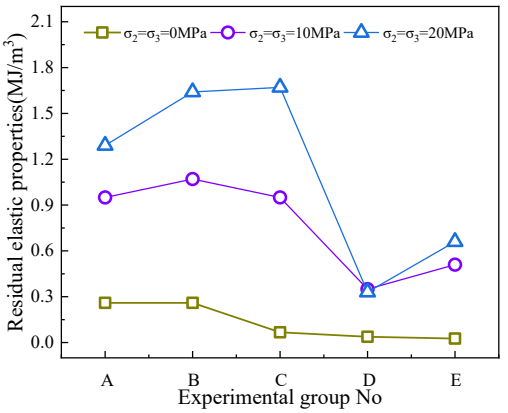

(b) Residual elastic performance

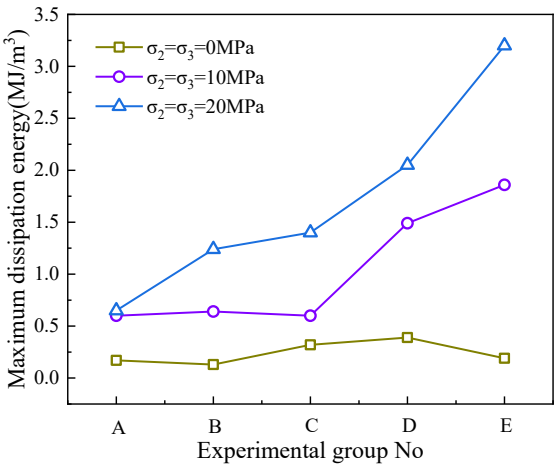

(c) Maximum dissipated energy

Fig. 13 Characteristic energy of samples in different experimental groups

It can be seen from the figure that under the same confining pressure, with the increase of microwave irradiation time, the characteristic energy value of low-power rock samples fluctuates more and the applied power decreases. For example, when the confining pressure is 20 MPa, the rock sample energy storage limits are 1.82, 1.83, 1.78, 1.56, and 2.59 MJ/m3, and the auxiliary amplitudes of low-power and high-power changes are 0.05 and 1.03, respectively. This reflects the fact that high-power irradiated specimens are more sensitive to changes in confining pressure. In addition, the maximum dissipation energy of high-power-irradiated rock samples under high confining pressure is higher than that at low power (the residual elastic energy (post-peak) is also lower).

6. CONCLUSION

1) Under microwave heating, with the increase of irradiation power and time, the sample density and P-wave velocity decrease. In a short period, the faster the temperature rise inside the sample under high-power irradiation, the greater the thermal stress difference between minerals. This is mainly reflected in the fact that, with the increase of the irradiation time, the sample density and P-wave velocity decrease under high-power irradiation is about 2.46 times faster than that at low-power.

2) Under the same confining pressure, the strength of the sample shows a downward trend with the increase of the irradiation time. The lower the confining pressure, the greater this change: the higher the irradiation power, the faster the strength decreases. As the confining pressure increases, the changes in the strength of the specimen under different microwave heating paths become more stable, reflecting the fact that the influence of microwave irradiation on the specimen decreases as the confining pressure increases.

3) The energy-storage limit and maximum energy dissipated of specimens are positively correlated with the confining pressure. Under the same confining pressure, with the increase of microwave irradiation time, the characteristic energy of low-power rock samples fluctuates to a greater extent and the power is smaller. This is closely related to the different mechanisms of fragmentation induced by microwave irradiation at different applied powers.

REFERENCES

[1] Li, X.B., Zhou, Z.L., Wang, W.H., The status and prospect of development in rock fragmentation engineering. 2009-2010 Report on Advances in Rock Mechanics and Rock Engineering. Beijing, China, 2010, p. 152-159 + 217-218.

[2] Haque, K.E., Microwave energy for mineral treatment processes--A brief review. International Journal of Mineral Processing, 1999, 57(1): p. 1-24.

[3] Ali, A. Y., & Bradshaw, S. M., Confined particle bed breakage of microwave treated and untreated ores. Minerals Engineering, 2011, 24(14): 1625-1630.

[4] Chen, T. T., Dutrizac, J. E., Haque, K. E., Wyslouzil, W., & Kashyap, S., The relative transparency of minerals to microwave radiation. Canadian Metallurgical Quarterly, 1984, 23(3): 349-351.

[5] Hartlieb, P., Leindl, M., Kuchar, F., Antretter, T., & Moser, P., Damage of basalt induced by microwave irradiation. Minerals Engineering, 2012, 31: 82-89.

[6] Hartlieb, P., Toifl, M., Kuchar, F., Meisels, R., & Antretter, T., Thermo-physical properties of selected hard rocks and their relation to microwave-assisted comminution. Minerals Engineering, 2016, 91: 34-41.

[7] Zhao, Q.H., Zhao, X.B., Zheng, Y.L., Li, J.C., He, L., Liu, H.W., Yu, J.W., A review on mineral heating characteristics and rock weakening effect under microwave irradiation. Geological Journal of China Universities, 2020, 26(3): p. 350-360.

[8] Zeng, J.S., Hu, Q.J., Chen, Y., Shu, X.Y., Chen, S.Z., He, L.P., Tang, H.X., Lu, X.R., Experimental investigation on structural evolution of granite at high temperature induced by microwave irradiation. Mineralogy and Petrology, 2019, 113: p. 745-754.

[9] Wei, W., Shao, Z.S., Zhang, Y.Y., Qiao, R.J., Gao, J.P., Fundamentals and Applications of Microwave Energy in Rock and Concrete Processing -A Review. Applied Thermal Engineering, 2019, 157: p. 113751.

[10] Farahat, M., Elmahdy, A.M., Hirajima, T., Influence of microwave radiation on the magnetic properties of molybdenite and arsenopyrite. Powder Technology, 2017, 315: p. 276-281.

[11] Estel, L., Poux, M., Benamara, N., Polaert, I., Continuous flowmicrowave reactor: Where are we. Chemical Engineering and Processing: Process Intensification, 2017, 113: p. 56-64.

[12] Batchelor, A. R., Jones, D. A., Plint, S., & Kingman, S. W., Deriving the ideal ore texture for microwave treatment of metalliferous ores. Minerals Engineering, 2015, 84: 116-129.

[13] Hartlieb, P., & Grafe, B. 2017. Experimental study on microwave assisted hard rock cutting of granite. BHM Berg- und Hüttenmännische Monatshefte, 162(2): 77-81.

[14] Peinsitt, T., Kuchar, F., Hartlieb, P., Moser, P., Kargl, H., Restner, U., & Sifferlinger, N., Microwave heating of dry and water saturated basalt, granite and sandstone. International Journal of Mining and Mineral Engineering, 2010, 21(1): p. 18-29

[15] Lu, G.M., Feng, X.T., Li, Y.H., Hassani, F., Zhang, X.W., Experimental Investigation on the Effects of Microwave Treatment on Basalt Heating, Mechanical Strength, and Fragmentation. Rock Mechanics and Rock Engineering, 2019, 52: p. 2535-2549.

[16] Lu, G.M., Feng, X.T., Li, Y.H., Zhang, X.W., The Microwave-Induced Fracturing of Hard Rock. Rock Mechanics and Rock Engineering, 2019, 52: p. 3017-3032.

[17] Lu, G.M., Li, Y.H., Hassani, F., Zhang, X.W., The influence of microwave irradiation on thermal properties of main rock-forming minerals. Applied Thermal Engineering, 2017, 112: p. 1523-1532.

[18] Nicco, M., Holley, E.A., Hartlieb, P., Kaunda, R., Nelson, P.P., Methods for Characterizing Cracks Induced in Rock. Rock Mechanics and Rock Engineering, 2018, 51: p. 2075-2093.

[19] Hassani, F., Nekoovaght, P.M., Gharib, N., The influence of microwave irradiation on rocks for microwave assisted underground excavation. Journal of Rock Mechanics and Geotechnical Engineering, 2016, 8(1): p. 1-15.

[20] Hassani, F., Nekoovaght, P.M., Radziszewski, P., Waters, K.E., Microwave assisted mechanical rock breaking. Proceedings of the 12th ISRM International Congress on Rock Mechanics. Beijing, China, 2011, p. 2075-2080

[21] Kingman, S.W., Vorster, W., Rowson, N.A., The influence of mineralogy on microwave assisted grinding. Minerals Engineering, 2000, 13(3): p. 313-327.

[22] Vorster, W., Rowson, N.A., Kingman, S.W., The effect of microwave radiation upon the processing of Neves Corvo copper ore. International Journal of Mineral Processing, 2001, 63(1): p. 29-44.

[23] Dai, J., Song, S.D., Tu, B.B., Gao, Y.Z., Du, W.P., Influence of granite strength under different microwave irradiation parameters. Science Technology and Engineering, 2017, 17(18): p. 188-192.

[24] Batchelor, A.R., Jones, D.A., Plint, S., Kingman, S.W., Deriving the ideal ore texture for microwave treatment of metalliferous ores. Minerals Engineering, 2015, 84: p. 116-129.

[25] Hartlieb, P., Toifl, M., Kuchar, F., Meisels, R., Antretter, T., Thermo-physical properties of selected hard rocks and their relation to microwave-assisted comminution. Minerals Engineering, 2016, 91: p. 34-41.

[26] Rizmanoski, V., The effect of microwave pretreatment on impact breakage of copper ore. Minerals Engineering, 2011, 24(14): p. 1609-1618.

[27] Toifl, M., Meisels, R., Hartlieb, P., Kuchar, F, Antretter, T., 3D numerical study on microwave induced stresses in inhomogeneous hard rocks. Minerals Engineering, 2016, 90: p. 29-42.

[28] Yang, J.M., Study on evolutionary mechanism of energy field and support mechanism of energy-absorbing bolt in deep roadway [D]. University of Science and Technology Beijing, 2020.

[29] Zhao, Z.H., Xie, H.P., Energy transfer and energy dissipation in rock deformation and fracture. Advanced Engineering Sciences, 2008, 40(02): p. 26-31.
[30] Xie, H.P., Ju, Y., Li, L.Y., Peng, R.D., Energy mechanism of deformation and failure of rock masses. Chinese Journal of Rock Mechanics and Engineering, 2008, 27(9): p. 1729-1740.